JPET Fast Forward. Published on May 13, 2011 as DOI: 10.1124/jpet.110.178012

Title Page:

Alpha-1 Adrenergic Receptors Positively Regulate Toll-Like Receptor Cytokine Production from Human Monocytes and Macrophages

Laurel A. Grisanti[1], Andrew P. Woster[2], Julie Dahlman, Edward R. Sauter, Colin K. Combs and James E. Porter

Department of Pharmacology, Physiology and Therapeutics (L.A.G., A.P.W., C.K.C., J.E.P.) and the Department of Surgery (J.D., E.R.S.)

University of North Dakota School of Medicine and Health Sciences

Grand Forks, North Dakota

Running Title Page:

a) Running Title:

α_1-AR Regulation of TLR4 Signaling in Monocyte/Macrophages

b) Corresponding Author:

James E. Porter

Department of Pharmacology, Physiology and Therapeutics

University of North Dakota School of Medicine and Health Sciences

501 North Columbia Road

Room 3700, Stop 9037

Grand Forks, ND 58202-9037

phone: (701) 777-4293

fax: (701) 777-4490

e-mail: james.porter@med.und.edu

c) Text Pages: 43

Tables: 1

Figures: 7

References: 40

Word Count for Abstract: 250

Word Count for Introduction: 695

Word Count for Discussion: 1492

JPET Fast Forward. Published on May 13, 2011 as DOI: 10.1124/jpet.110.178012
This article has not been copyedited and formatted. The final version may differ from this version.

d) Nonstandard Abbreviations:

AR, adrenergic receptor

Bis II, bisindolylmaleimide II

B_{max}, specific binding site density

BMY 7378, 8-[2-[4-(2-Methoxyphenyl)-1-piperazinyl]ethyl]-8-azaspiro[4.5]decane-7,9-dione dihydrochloride

DN, dominant-negative

EGTA, ethylene glycol tetraacetic acid

ELISA, enzyme-linked immunosorbent assay

FBS, fetal bovine serum

BE 2254, 2-{[*β*-(hydroxyphenyl)ethyl]aminomethyl}-1-tetralone hydrochloride

HEPES, 4-(2-hydroxyethyl)-1-piperazineethanesulfonic acid

^{125}I-HEAT, (±)-β-([^{125}]Iodo-4-hydroxyphenyl)-ethyl-aminomethyl-tetralone

IL, interleukin

K_d, radioligand equilibrium dissociation constant

K_i, competitive receptor antagonist equilibrium dissociation constant

LPS, lipopolysaccharide

MAPK, mitogen-activated protein kinase

5-MU, 5-methylurapidil

PE, (R)-(-)-phenylephrine hydrochloride

PEI, polyethylenimine

PKC, protein kinase C

JPET Fast Forward. Published on May 13, 2011 as DOI: 10.1124/jpet.110.178012
This article has not been copyedited and formatted. The final version may differ from this version.

PMA, phorbol 12-myristate 13-acetate

SB 203580, 4-(4-Fluorophenyl)-2-(4-methylsulfinylphenyl)-5-(4-pyridyl)-1H-imidazole

STS, staurosporine

TAK1, transforming growth factor β-activated kinase 1

THP-1, human monocyte cell line

TLR, Toll-like receptor

TNF, tissue necrosis factor

WB-4101, 2-[(2,6-Dimethoxyphenoxyethyl)aminomethyl]-1,4-benzodioxane hydrochloride

e) Recommended Section Assignment:

Inflammation, Immunopharmacology and Asthma

Abstract:

Catecholamines released from the sympathetic nervous system in response to stress or injury impact expression of inflammatory cytokines generated by immune cells. α_1-Adrenergic receptors (AR) are expressed on innate immune cell populations, but their subtype expression patterns and signaling characteristics are not well characterized. Primary human monocytes, a human monocytic cell line and monocyte-derived macrophage cells were used to measure expression of the pro-inflammatory mediator interleukin (IL)-1β responding to lipopolysaccharide (LPS) in the presence or absence of α_1-AR activation. Based on our previous findings, we hypothesized that α_1-AR stimulation on innate immune cells positively regulates LPS initiated IL-1β production. IL-1β production in response to LPS was synergistically higher for both monocytes and macrophages in the presence of the selective α_1-AR agonist, phenylephrine (PE). This synergistic IL-1β response could be blocked with a selective α_1-AR antagonist as well as inhibitors of protein kinase C (PKC). Radioligand binding studies characterized a homogenous α_{1B}-AR subtype population on monocytes, which changed to a heterogeneous receptor subtype expression pattern when differentiated to macrophages. Furthermore, increased p38 mitogen-activated protein kinase (MAPK) activation was observed only with concurrent PE and LPS stimulation, peaking after 120 and 30 min in monocytes and macrophages, respectively. Blocking the PKC/p38 MAPK signaling pathway in both innate immune cell types inhibited the synergistic IL-1β increase observed with concurrent PE and LPS treatments. This study characterizes α_1-AR subtype expression on both human monocyte as well as macrophage cells and illustrates a mechanism by which increased IL-1β production can be modulated by α_1-AR input.

Introduction:

The innate immune system is important as the first line of defense against a pathological challenge or damage to tissue. It comprises a group of cells and other mechanisms that act as the body's first means of protection against infection or irritation, working to remove the injurious stimuli and promote healing. The sympathetic nervous system is an important regulatory mechanism for the innate immune response. Specifically, production of the endogenous catecholamines epinephrine and norepinephrine are increased during times of anxiety, pathogenic challenge or injury and are known to play a role in many physiological responses including alteration of the innate immune response (Calcagni and Elenkov, 2006). For example, norepinephrine has been shown to have a variety of effects on innate immune responses including alteration of cytokine levels following a bacterial endotoxin challenge (Elenkov et al., 2008). Moreover, prolonged stimulation of the sympathetic nervous system leads to increased inflammation with a corresponding decrease in the ability to fight infections (Johnson et al., 2005). Also, in many chronic inflammatory diseases such as rheumatoid arthritis and multiple sclerosis, increased sympathetic activity is correlated with a heightened disease progression (Brosnan et al., 1985; Capellino and Straub, 2008). Understanding how sympathetic input regulates innate immune cytokine production may prove useful in treating or slowing the progression of these and many other chronic inflammatory disorders.

Effects of epinephrine and norepinephrine are mediated through three AR families that are further characterized into nine receptor subtypes (α_{1A}, α_{1B}, α_{1D}, α_{2A}, α_{2B}, α_{2C}, β_1, β_2, and β_3; see review by Guimarães and Moura, 2001)). All three AR families are found to be expressed on many types of immunocompetent cells involved with innate immune responses and are generally

thought to play an anti-inflammatory role. For example, activation of α_2- or β-AR types have been shown to be responsible for many anti-inflammatory immune cell responses observed after norepinephrine treatment (Farmer and Pugin, 2000; Romero-Sandoval et al., 2005). However, increasing evidence is found in the literature characterizing increased cytokine production by α_2-AR stimulation (Spengler et al., 1990; Felsner et al., 1995; Hasko et al., 1995; Flierl et al., 2007) or modified by selective β-AR activation (Grisanti et al., 2010). This demonstrates the importance for determining AR expression profiles from a finite cell population that correspond to specific immune responses. Immunomodulatory α_1-AR characteristics are the least studied of all three AR families. α_1-AR stimulation appears to possess a pro-inflammatory effect on immune system responses, which is correlative to many chronic inflammatory disease states (Maestroni, 2000; Heijnen et al., 2002; Perez et al., 2009). For example, in children with polyarticular juvenile rheumatoid arthritis, α_1-AR expression on peripheral blood mononuclear cells is responsible for increasing production of the pro-inflammatory cytokine IL-6 (Heijnen et al., 1996). Other investigations have implicated α_1-AR activation to be important for increasing inflammatory responses in an established model of multiple sclerosis (Brosnan et al., 1985). Therefore, understanding α_1-AR mechanisms that modulate innate immune cytokine production is perhaps important for the development of therapeutic strategies that would selectively regulate inflammatory responses in diseases for which immunocompetent cells play an essential pathological function.

Based on our previous findings in which cytokine/chemokine changes from human monocytes following simultaneous α_1-AR and Toll-like receptor (TLR) 4 stimulation were screened using an antibody array, we investigated the hypothesis that α_1-AR modulated innate immune

responses have pro-inflammatory outcomes, which are dependent upon the selective signaling characteristics of α_1-AR subtypes expressed on immunocompetent cells (Grisanti et al., in press). Using primary and immortalized (THP-1) human monocytes as a monocytic model system as well as phorbol 12-myristate 13-acetate (PMA) differentiated THP-1 cells as a monocyte-derived macrophage cell model (Tsuchiya et al., 1982), we examined effects of concurrent α_1-AR stimulation on LPS-induced inflammatory responses. LPS is a component of the Gram negative bacterial cell wall that activate TLR4 subtypes expressed on immunocompetent cells, which leads to the production of many pro-inflammatory cytokines including IL-6, IL-8, IL-1β and tissue necrosis factor (TNF)-α. Our results not only document a unique switching of α_1-AR subtype expression during myeloid cell development, but are also the first to demonstrate a mechanism for α_1-AR mediated increases in IL-1β generation from immunocompetent cells that have been pathogenically challenged to initiate an inflammatory response.

JPET Fast Forward. Published on May 13, 2011 as DOI: 10.1124/jpet.110.178012
This article has not been copyedited and formatted. The final version may differ from this version.

Methods:

Materials:

Bisindolylmaleimide II (Bis II), LPS (cat #L2654; *E. coli* serotype O26:B6), (R)-(-)-phenylephrine hydrochloride (PE), staurosporine (STS), PMA, phentolamine, [2-[(2,6-dimethoxyphenoxyethyl)aminomethyl]-1,4-benzodioxane hydrochloride] (WB-4101), 4-(4-Fluorophenyl)-2-(4-methylsulfinylphenyl)-5-(4-pyridyl)-1H-imidazole (SB 203580), 5-methylurapidil (5-MU), benzamidine, leupeptin, phenylmethylsulfonyl fluoride and bacitracin were obtained from Sigma-Aldrich (St. Louis, MO). [8-[2-[4-(2-methoxyphenyl)-1-piperazinyl]ethyl]-8-azaspiro[4.5]decane-7,9-dione dihydrochloride] (BMY 7378) and 2-{[*β*-(hydroxyphenyl)ethyl]aminomethyl}-1-tetralone hydrochloride (BE 2254) were purchased through Tocris Bioscience (Ellisville, MO). (±)-β-([^{125}]Iodo-4-hydroxyphenyl)-ethyl-aminomethyl-tetralone (^{125}I-HEAT) was ordered through Perkin Elmer (Waltham, MA). All other buffers and chemical reagents were of biological grade purchased through Thermo-Fisher Scientific (Rockford, IL).

Cell Culture:

THP-1 cells (ATCC, Manassas, VA) were cultured in RPMI-1640 medium (HyClone, Waltham, MA) with 2 mM L-glutamine adjusted to contain 1.5 g/L sodium bicarbonate, 4.5 g/L glucose and 10 mM HEPES (complete media), supplemented with 10% heat inactivated fetal bovine serum (FBS; Atlanta Biologicals, Atlanta, GA) under standard cell culture growth conditions (37° C/5% CO_2/95% humidified air). To differentiate monocytes into macrophages, THP-1 cells were treated with 200 nM PMA 48 h prior to all experiments. Cells ($1x10^6$ per treatment group) were washed with serum-free complete media 30 min prior to experiments and allowed to

become quiescent before preincubation with receptor antagonists (1 h, 500 nM BE 2254) or kinase inhibitors (1 h, 10 nM STS; 1 h, 200 nM Bis II; 16 h, 1 μM SB 203580) followed by treatment with the selective α_1-AR agonist, PE (10 μM) and/or the TLR4 agonist, LPS (25 ng/mL). Preliminary temporal studies were performed to ascertain a time point (3 h) where significant amounts of IL-1β were generated in response to LPS. Final drug concentrations were based on affinity values calculated from competition binding curves (BE 2254), preliminary concentration-response experiments (PE, LPS) or IC_{50} values of chemical inhibitors (STS, Bis II, SB 203580). Immunocompetent cell viability was assessed by trypan blue exclusion staining. Greater than 99% cell viability was observed for all treatments after 3 or 24 h and did not significantly differ between experimental groups (data not shown).

Isolation of Primary Human Monocytes:

The lymphocyte layer was obtained from the peripheral blood of healthy adults. Briefly, human monocytes were separated by centrifugation at 600 x *g* for 20 min at 22° C using a 30-45-60% Percoll density gradient. The monocyte-enriched fraction was removed from the 30-45% gradient interface, washed then re-suspended in complete media containing 10% heat inactivated FBS and incubated overnight under standard cell culture growth conditions. $1x10^6$ cells/mL were washed in serum-free complete medium and allowed to become quiescent for 30 min prior to the addition of PE (10 μM) and/or LPS (25 ng/mL).

Membrane Preparation for Receptor Binding

A crude membrane preparation was performed on untreated THP-1 cells and PMA differentiated THP-1 cells as previously described (Grisanti et al., 2010). In short, cells were collected in a 50

JPET Fast Forward. Published on May 13, 2011 as DOI: 10.1124/jpet.110.178012
This article has not been copyedited and formatted. The final version may differ from this version.

mL conical tube, followed by two washings at 500 x g using cold Hank's balanced salt solution (HBSS). Cells were then re-suspended in water containing a protease inhibitor cocktail (10 μg/mL benzamidine, 10 μg/mL leupeptin, 20 μg/mL phenylmethylsulfonylfloride and 10 μg/mL bacitracin). The cells were disrupted by freezing at -80˚ C for 20 min followed by homogenization of the thawed suspension using 25 strokes from a loose fitting Dounce homogenizer (B) pestle. The mixture was then centrifuged at 2100 x g for 15 min to remove nuclear debris. Following centrifugation, HEM buffer (20 mM HEPES, 1.4 mM EGTA, 12.5 mM $MgCl_2$, pH 7.4) was added and the mixture re-centrifuged at 30,000 x g for 15 min. The final pellet was re-suspended in HEM buffer containing 10% glycerol and stored at -80˚ C until used for radioligand binding. Protein concentrations were determined using the method of Bradford described previously (Grisanti et al., 2010).

Radioligand Binding:

Radioligand binding was performed using crude THP-1 or PMA-differentiated THP-1 cell membranes as previously described (Grisanti et al., 2010). Briefly, saturation binding experiments were performed using the selective α_1-AR radioligand antagonist, ^{125}I-HEAT. Cell membranes were allowed to equilibrate for 1 h at 37° C with increasing concentrations of ^{125}I-HEAT (0.5-0.01 nM) in a 250 μL total volume of HEM buffer. A saturable concentration (100 μM) of the α-AR antagonist, phentolamine was used to determine non-specific binding. Total binding was stopped by filtering the equilibrated cell membranes through Whatman GF/B filters that had been soaked in 0.1% bovine serum albumin (BSA) and 0.3% polyethylenimine (PEI) to reduce non-specific binding to the filter. This was followed by washing the membrane bound filter five times with 5 mL of cold (4° C) HEM buffer to remove any unbound drug. Total and

JPET Fast Forward. Published on May 13, 2011 as DOI: 10.1124/jpet.110.178012
This article has not been copyedited and formatted. The final version may differ from this version.

non-specific binding to cell membrane preparations was determined from the remaining radioactive counts. CPM values were plotted as a function of the ^{125}I-HEAT concentration and from each rectangular hyperbola, specific binding site densities (B_{max}) as well as the equilibrium dissociation constant (K_d) of ^{125}I-HEAT for these putative α_1-ARs was calculated using non-linear regression analysis (GraphPad Prism version 5.04 for Windows, GraphPad Software, San Diego California USA, www.graphpad.com). Competitive radioligand binding was performed using a single concentration (0.1 nM) of ^{125}I-HEAT with increasing concentrations of the selective α_1-AR antagonist BE 2254 or the subtype-selective α_1-AR antagonists 5-MU, WB-4101 and BMY 7378 in a 250 μL total volume of HEM buffer. Specific radioactive counts were plotted as a function of the competitive receptor antagonist concentration and non-linear regression analysis was used to determine the concentration of receptor antagonist that reduced specific ^{125}I-HEAT binding by 50% (IC_{50}). Equilibrium dissociation constants (K_i) of each competitive α_1-AR antagonist for specific ^{125}I-HEAT binding sites were calculated using the method of Cheng and Prusoff as previously described (Grisanti et al., 2010).

Plasmids and Transfections

A dominant-negative (DN) p38 MAPK and empty vector DNA plasmid constructs have been described previously (Whitmarsh et al., 1995) and kindly provided by Dr. Philip Howe (The Cleveland Clinic Foundation, Cleveland, OH). THP-1 cells were individually transfected with DN p38 MAPK or empty vector constructs ($5x10^6$ cells/0.5 μg DNA) by electroporation using the Amaxa Nucleofector system according to manufacturer's instructions (Amaxa Inc., Gaithersburg, MD). 48 h following transfection, cells were treated 3 h with PE (10 μM) and/or LPS (25 ng/mL) and subsequently lysed for immunoblot analysis.

Immunoblot Hybridization

Following drug treatments, an equal number of cells were lysed using a modified radioimmunoprecipitation assay (RIPA) buffer (150 mM NaCl, 10 mM Tris, pH 7.2, 0.1% sodium dodecylsulphate, 1.0% Triton X-100, 1.0% sodium deoxycholate, 5 mM EDTA) containing 1.0% protease and phosphatases inhibitor cocktails (Sigma-Aldrich, St. Louis, MO). Equal amounts of total cell lysates were resolved by SDS-PAGE (12% for IL-1β and 10% for MAPK analysis) then transferred to polyvinylidene difluoride (PVDF) membranes (Millipore, Billerica, MA). Polyacrylamide gels were loaded with 60 or 20 μg protein/well for IL-1β and MAPK immunoblots, respectively. Expression was measured by immunoblotting overnight at 4° C with diluted antibodies against human IL-1β (2 μg/mL; R&D Systems, Minneapolis, MN), extracellular signal-regulated kinase (ERK, 1:1000; Cell Signaling, Danvers, MA), phospho-ERK (1:1000; Cell Signaling, Danvers, MA), c-Jun N-terminal kinase (JNK, 1:1000; Cell Signaling, Danvers, MA), phospho-JNK (1:1000; Cell Signaling, Danvers, MA), phopho-p38 (1:1000; Cell Signaling, Danvers, MA), p38 (1:1000; Cell Signaling, Danvers, MA), α_{1A}-AR (1:1000; Santa Cruz Laboratories, Santa Cruz, CA), α_{1B}-AR (1:1000; Santa Cruz Laboratories, Santa Cruz, CA), α_{1D}-AR (1:1000; Santa Cruz Laboratories, Santa Cruz, CA) or actin (1:1000; Santa Cruz Laboratories, Santa Cruz, CA). After washing, PVDF membranes were incubated at 22 °C for 90 min with the appropriate diluted horseradish peroxidase-linked secondary antibody (1:5000; Jackson ImmunoResearch, West Grove, PA). Bound antibody was visualized by chemiluminescent imaging (Thermo-Fisher Scientific, Rockford, IL) and documented by digital photography (UVP, Upland, CA). Pixel values were normalized to β-actin or non-

phosphorylated MAPK and compared with basal expression levels. Protein concentrations were measured using the method of Bradford described previously (Grisanti et al., 2010).

Enzyme-Linked Immunosorbent Assay (ELISA)

Following drug treatment, an equal number of THP-1 cells were centrifuged at 600 x g for 5 min to pellet the cells. The supernatant was then collected and stored at -20° C until use for ELISA. Concentrations of IL-1β in the culture media were determined using the human IL-1β/IL-1F2 Quantikine HS ELISA (R&D Systems, Minneapolis, MN) according to manufacturer's instructions. The minimal and maximal IL-1β detection limit of the standard curve ran with each ELISA was 0.06 and 8 pg/mL, respectively.

Statistical Analyses

A Wald-Wolfowitz runs test was used to determine if the data differed significantly from a linear relationship ($p < 0.05$). For each experiment, the fitted iterative nonlinear regression curve that best represented the data was determined using a partial f test ($p < 0.05$). Significance among groups was tested using an unpaired t test or one-way analysis of variance followed by a Tukey's multiple comparison test ($p < 0.05$). All values are reported as the mean ± S.E.M. of n experiments, performed in duplicate. Each n represents an individual experiment from an independent cell preparation or passage.

JPET Fast Forward. Published on May 13, 2011 as DOI: 10.1124/jpet.110.178012
This article has not been copyedited and formatted. The final version may differ from this version.

Results:

α_1-AR stimulation increases IL-1β production in human monocytes responding to LPS. We first sought to determine the *ex vivo* effects of simultaneous α_1-AR activation on inflammatory cytokine responses generated by pathogenically primed primary monocytes isolated from human blood. Based on our previous report (Grisanti et al., in press), primary monocytes were treated for 3 h with LPS in the presence or absence of PE, then probed for changes in the level of IL-1β production (fig 1, panels A-B). Immunoblot analysis showed no change from basal in IL-1β generation for primary monocytes treated with PE alone (fig 1, panel B, lane 2). However, an anticipated significant ($p < 0.05$) increase over basal in generated IL-1β was observed for cells treated with LPS only (fig 1, panel B, lane 3). More importantly, an unexpected synergistic increase in IL-1β production is shown from cells treated concurrently with PE and LPS, which was significantly different ($p < 0.05$) from both control and LPS only treatments (fig 1, panel B, lane 4).

In order to confirm our *ex vivo* findings and establish an *in vitro* monocyte model system for further receptor-signal transduction investigations, THP-1 cells were treated in the same manner as described for primary human monocytes. Resolved THP-1 cell lysates were then probed for changes in IL-1β production (fig 2, panels A-B). Immunoblot analysis again showed no change from basal in generated IL-1β from THP-1 cells treated with PE alone (fig 2, panel B, lane 2). Similarly, a significant ($p < 0.05$) increase over basal in IL-1β production was observed for cells treated with LPS only (fig 2, panel B, lane 3). Moreover, a synergistic increase in IL-1β production was observed from cells treated with both PE and LPS, which was significantly different ($p < 0.05$) from both control and LPS only treatments (fig 2, panel B, lane 4). In

addition, this PE-immunomodulatory IL-1β response was blocked in the presence of the selective α_1-AR antagonist BE 2254, to levels that were significantly ($p < 0.05$) different from control as well as concurrent PE and LPS treatments (fig 2, panel B, lane 5). However, IL-1β amounts were similar to levels generated using LPS only, indicating a specific α_1-AR-mediated event. Treatment of cells with BE 2254 alone showed no difference in IL-1β amounts from control (fig 2, panel B, lane 6).

To test the hypothesis that α_1-AR modulation of IL-1β production in LPS-challenged monocytes is mediated through classical $G\alpha_q$-initiated signal transduction pathways, we pretreated with the non-specific PKC inhibitor STS (fig 2, panels A-B). Synergistic increases in IL-1β production were not observed in lysates from cells pretreated with STS followed by concurrent PE and LPS incubation (fig 2, panel B, lane 7). However, the measured amount of IL-1β generated was significantly different ($p < 0.05$) from control and similar to levels observed with LPS alone. Furthermore, pretreatment with STS alone did not change IL-1β amounts when compared to control (fig 2, panel B, lane 8).

Pro-IL-1β processing into the bioactive 17-kDa secreted form is a result of constitutive caspase-1 activation through a one-time stimulation of TLR4 receptors (Netea et al., 2009). As a result, we expect that heighted pro-IL-1β generation observed from treated monocytic cell lysates will correlate to the same increase of secreted cytokine. To test this hypothesis the amount of secreted IL-1β was quantified using ELISA analysis from conditioned media of treated THP-1 cells (fig 2, panel C). Similar to results quantifying levels of pro-IL-1β (32 kDa) using immunoblot analysis, there were no changes in amounts of secreted IL-1β from cells treated with

PE alone (fig 2, panel C, lane 2). However, there were significant ($p < 0.05$) increases in amounts of IL-1β secreted from LPS only treated cells when compared with control (fig 2, panel C, lane 3). More importantly, we observed a synergistic IL-1β increase from the media of cells treated with PE plus LPS, which was significantly ($p < 0.05$) different from amounts secreted basally or from LPS only treatment (fig 2, panel C, lane 4).

Concurrent PE and LPS stimulation leads to PKC-dependent p38 MAPK phosphorylation in human monocytes and macrophages. α_1-AR stimulation has been shown to increase MAPK activity leading to greater pro-inflammatory cytokine production from fibroblasts (Perez et al., 2009). Therefore, we wanted to determine if monocyte MAPK pathways were being activated by α_1-AR agonists in the presence of LPS. Temporal responses of THP-1 cells treated with LPS alone or simultaneously with PE and LPS over a period of 3 h were performed then analyzed for MAPK activation (fig 3, panels A-C). No temporal differences above basal for phosphorylated ERK or JNK were observed from monocytes stimulated with LPS only or concomitantly with PE and LPS (data not shown). Conversely, p38 MAPK was temporally phosphorylated at significant ($p < 0.05$) levels 30 min after simultaneous PE and LPS treatment, with peak activation occurring at 2 h (fig 3, panels A-B). This response was specific for concurrent α_1-AR and TLR4 stimulation because activation of p38 MAPK was not observed at any time point for cells treated with LPS alone (fig 3, panel C). Further assessments of p38 MAPK activation in monocytes were subsequently evaluated after a 2 h treatment with receptor agonists.

We also wanted to determine if α_1-AR activation initiates p38 MAPK in human monocyte-derived macrophages. Therefore, temporal responses of PMA differentiated THP-1 cells to

treatments of PE and/or LPS were performed over a period of 2 h (fig 3, panels D-F). No temporal differences in phosphorylated ERK or JNK were observed from macrophages individually or concomitantly treated with PE and LPS when compared to control (data not shown). Conversely, p38 MAPK was temporally phosphorylated at significant ($p < 0.05$) levels above basal starting 15 min after concurrent treatment with PE and LPS, with peak activation occurring at 30 min (fig 3, panels D-E). Moreover, activation of p38 MAPK in macrophages was not observed at any time point using LPS alone (fig 3, panel F). Subsequent assessment of p38 MAPK activation in macrophages was evaluated after a 30 min receptor agonist treatment.

To directly associate α_1-AR stimulation to p38 MAPK activation in LPS-challenged monocytes and macrophages, we preincubated with the selective inhibitor SB 203580 (fig 4, panels A-D). Immunoblot analysis showed no changes from basal in the generation of phospho-p38 from cells individually treated with PE or LPS alone (fig 4, panels B&D, lanes 2-3). However, there was significant ($p < 0.05$) increases in phospho-p38 production observed from cells simultaneously treated with PE and LPS when compared with control (fig 4, panels B&D, lane 4). Moreover, this increased phospho-p38 MAPK could be blocked to similar levels as control by preincubation with SB 203580 (fig 4, panels B&D, lane 5). In parallel experiments, pretreatment with the selective PKC inhibitor Bis II, completely inhibited phospho-p38 MAPK generation in the presence of concurrent PE and LPS treatment, to levels that were no different from control (fig 4, panels B&D, lane 7). Treatment of cells with SB 203580 or Bis II alone did not alter phospho-p38 MAPK basal levels (fig 4, panels B&D, lanes 6&8).

JPET Fast Forward. Published on May 13, 2011 as DOI: 10.1124/jpet.110.178012
This article has not been copyedited and formatted. The final version may differ from this version.

Synergistic IL-1β production in human monocytes and macrophages is associated with a PKC/p38 MAPK-dependent mechanism. To test whether the synergistic IL-1β response caused by α_1-AR stimulation in LPS-challenged monocytes and macrophages is coupled through PKC/p38 MAPK activation we again preincubated with the selective inhibitors SB 203580 and Bis II (fig 5, panels A-D). Immunoblot analysis showed no basal differences in the amount of IL-1β generated from cells treated with PE alone as well as the expected significant ($p < 0.05$) increase from cells treated with LPS only (fig 5, panels B&D, lanes 2-3). In addition, synergistic production of IL-1β was observed from cells concurrently treated with PE and LPS, which was significantly ($p < 0.05$) greater than amounts generated basally and with LPS alone (fig 5, panels B&D, lane 4). Cells preincubated with SB 203580 showed no IL-1β differences from levels produced with LPS alone. However, SB 203580 preincubated cells displayed significant ($p < 0.05$) changes in generated IL-1β when compared to control or concurrent PE and LPS treatments (fig 5, panels B&D, lane 5). In parallel experiments, cells preincubated with Bis II showed significant ($p < 0.05$) modifications of generated IL-1β (fig 5, panels B&D, lane 7). Amounts of IL-1β from cells treated with SB 203580 or Bis II alone were no different from basal (fig 5, panels B&D, lanes 6&8).

We also applied a molecular biological approach using a previously described DN form of p38 MAPK to corroborate our results using p38 MAPK pharmacological inhibitors (Whitmarsh et al., 1995). Figure 6 shows results from immunoblot analysis of resolved THP-1 cell lysates that had been transfected with either empty vector or the DN p38 MAPK plasmid construct followed by concurrent treatment with PE and LPS. For both sets of transfected cells there was the expected ≈ 3-fold increase of generated IL-1β over basal in the presence of LPS alone with no differences

from control after treatment with PE only (data not shown). Moreover, there were significant ($p < 0.05$) increases in amounts of IL-1β produced from cells transfected with the empty vector then treated simultaneously with PE and LPS when compared with control (fig 6, lane 2). Conversely, cells transfected with the DN p38 MAPK plasmid construct then concurrently treated with PE and LPS showed no differences in amounts of IL-1β generated when compared to basal expression from similarly transfected cells (fig 6, lanes 3-4).

Characterization of α_1-AR subtype expression on human monocytes and macrophages. Genomic α_1-AR subtype expression patterns have previously been reported for human monocytes, however we were interested in subtype characteristics of the mature membrane protein (Rouppe van der Voort et al., 1999; Heijnen et al., 2002). We initially probed lysates from non-stimulated THP-1 cells with commercial antibodies whose epitopes were selectively generated for each α_1-AR subtype. Shown in figure 7 are the results from 3 independent lysate preparations probed with subtype-selective α_{1A}- and α_{1B}-AR antibodies. Resolved lysates probed with the α_{1B}-AR antibody were the only immunoblots that showed somewhat consistent weak specific banding at the expected size of ≈ 88 kDa, although numerous non-specific bands were also identified. Conversely, membranes immunoblotted with the selective α_{1A}-AR antibody showed no specific banding at the expected size of the mature membrane protein. Similar non-specific results were also found when probing THP-1 cell lysates with the subtype-selective α_{1D}-AR antibody (data not shown).

To reliably characterize α_1-AR subtype expression on human monocytes we used the iodinated α_1-AR antagonist ^{125}I-HEAT to identify specific binding sites on untreated THP-1 cell membrane

JPET Fast Forward. Published on May 13, 2011 as DOI: 10.1124/jpet.110.178012
This article has not been copyedited and formatted. The final version may differ from this version.

preparations. ^{125}I-HEAT labeled a saturable, homogenous and specific high affinity binding site on THP-1 membranes with a total site number (B_{max}) of 309±72 fmol/mg protein (*n*=4; data not shown). The equilibrium dissociation constant (K_d) of ^{125}I-HEAT calculated for these specific binding sites was 632±234 pM (*n*=4), which is similar to ^{125}I-HEAT affinity values used to identify α_1-AR specific binding sites in other systems (Goetz et al., 1995). Competition binding assays were also performed using selective α_1-AR antagonists. Table 1 summarizes affinity values calculated from individually generated inhibition curves using these α_1-AR antagonists to compete for specific monocyte ^{125}I-HEAT binding sites. When the selective α_1-AR antagonist, BE 2254, was used to compete for specific radiolabeled binding sites, a one-site competition curve was best fit to the data with a calculated equilibrium dissociation constant (K_i) of 5.3±1.0 nM (*n*=3). This value corresponds to the K_d of the analogous iodinated compound (^{125}I-HEAT) and is similar to the calculated affinity of BE 2254 when used to identify α_1-AR binding sites in other membrane preparations (Goetz et al., 1995). Subtype-selective α_1-AR antagonists were used to establish the characteristics of these monocyte α_1-AR binding sites. A one-site model fit best when the α_{1A}-AR subtype-selective antagonists 5-methylurapadil (5-MU) or WB-4101 as well as the α_{1D}-AR subtype-selective antagonist BMY 7378 were used to competitively displace specific monocyte ^{125}I-HEAT binding sites. The low affinity estimates of 5-MU, WB-4101 and BMY 7378 for specific monocyte ^{125}I-HEAT binding sites do not correspond with the high affinity values of these subtype-selective α_1-AR antagonists calculated for the α_{1A}- or α_{1D}-AR in other systems (Gross et al., 1988; Goetz et al., 1995).

To determine if this characterized α_1-AR subtype expression pattern is retained in monocyte-derived macrophages, radioligand binding studies were performed on membranes prepared from

PMA differentiated THP-1 cells. Subsequent radioligand saturation binding analysis on these macrophage membrane preparations documented a saturable, homogenous and specific high affinity ^{125}I-HEAT binding site (data not shown). The number of specific binding sites was calculated to be 97±32 fmol/mg protein and the estimated K_d of ^{125}I-HEAT for these macrophage binding sites was 468±67 pM (*n*=4). This calculated ^{125}I-HEAT affinity for specific macrophage binding sites is similar to estimated K_d values which identified α_1-AR populations on monocytes and in other systems (Goetz et al., 1995). Competition binding assays were also performed using the subtype-selective α_1-AR antagonists, 5-MU and BMY 7378 (table 1). Both receptor antagonists competitively displaced specific ^{125}I-HEAT binding sites on macrophage membranes that best fit a two-site model, suggesting a heterogeneous α_1-AR subtype profile.

Discussion:

Based on previous studies, we hypothesized that α_1-AR modulation of TLR4 responses would have pro-inflammatory outcomes dependent upon the selective signaling characteristics of expressed α_1-AR subtypes (Grisanti et al., in press). In agreement with our findings, α_1-AR activation appears to play a pro-inflammatory role in many situations. For example, α_1-AR expression is increased in several animal models of chronic human diseases with known inflammatory etiologies such as juvenile rheumatoid arthritis and multiple sclerosis (Brosnan et al., 1985; Capellino and Straub, 2008). Other studies from juvenile rheumatoid arthritis patients have linked heightened α_1-AR expression on peripheral blood leukocytes to an increased production of the pro-inflammatory cytokine, IL-6, when stimulated with PE (Heijnen et al., 1996). Similarly, in this report we characterized α_1-AR mediated synergistic increases in IL-1β levels from LPS-challenged human monocytes (fig 1). We used immunoblot analysis to quantitate pro-IL-1β production as a measure of this synergistic α_1-AR response. Differences in IL-1β levels, as measured by ELISA, from conditioned media of LPS alone and LPS plus PE treated monocytes, were comparable (≈ 3-fold) to differences observed for pro-IL-1β generation in similarly treated cells (fig 2). These results correlate quantitation of bioactive IL-1β secreted into the media to the same levels of pro-cytokine generation using immunoblot analysis, validating use of this latter technique in our studies. Furthermore, α_1-AR-mediated synergistic effects between primary and immortalized monocytes were similar (≈ 3-fold) when compared with LPS treatment alone (figs 1-2). This observation is analogous to previously described potentiated IL-1β responses caused by simultaneous stimulation of TLR4 and β_1-AR subtypes in both primary monocytes and THP-1 cells (Grisanti et al., 2010) and justifies use of these immortalized cells for subsequent signal transduction investigations.

JPET Fast Forward. Published on May 13, 2011 as DOI: 10.1124/jpet.110.178012
This article has not been copyedited and formatted. The final version may differ from this version.

Previous studies using radioligand binding analysis documented no specific α_1-AR binding from a human mononuclear cell preparation, attributing earlier reports describing α_1-AR activity, to platelet contamination (Casale and Kaliner, 1984). Subsequent investigations have identified genomic expression of α_{1B}- and α_{1D}-AR subtypes from THP-1 total RNA preparations, however, mature translational expression was not examined (Rouppe van der Voort et al., 1999). α_1-AR expression in the immune system has been shown to be increased by neuroendocrine mediators such as glucocorticoids, cytokines and β-AR stimulation (Rouppe van der Voort et al., 1999; Rouppe van der Voort et al., 2000; Heijnen et al., 2002). Activation of TLR4 in our model system may induce α_1-AR expression, which could explain why many researchers did not previously detect α_1-AR specific binding. Nonetheless, our studies document mature α_1-AR expression from non-stimulated human monocyte and macrophage cell preparations (table 1). Commercial subtype-selective α_1-AR antibodies have been reported to be non-specific when tested in genetically modified animals (Jensen et al., 2009). Therefore, radioligand binding assays remain the only consistent method of quantitating α_1-AR expression. We described a one-site, low affinity profile of the selective α_{1A}-AR antagonists 5-MU and WB-4101 for specific ^{125}I-HEAT binding sites on untreated monocyte membranes, suggesting expression of the α_{1B}- or α_{1D}-AR subtype. One-site, low affinity values of the selective α_{1D}-AR antagonist for specific ^{125}I-HEAT binding sites on these same preparations, indicates the absence of mature α_{1D}-AR subtypes, which reinforces our conclusions for homogenous α_{1B}-AR protein expression yet contrasts previous reports characterizing α_{1D}-AR transcripts from monocytes (Rouppe van der Voort et al., 1999).

JPET Fast Forward. Published on May 13, 2011 as DOI: 10.1124/jpet.110.178012
This article has not been copyedited and formatted. The final version may differ from this version.

In macrophages, a two-site, high and low affinity profile of 5-MU was calculated for specific ^{125}I-HEAT binding sites, confirming mature expression of the α_{1A}-AR and suggesting the presence of α_{1B}- or α_{1D}-AR subtypes. A similar two-site, high and low affinity profile of BMY 7378 was calculated for specific ^{125}I-HEAT binding sites on these same cells, which confirms mature expression of the α_{1D}-AR and validates our α_{1A}-AR subtype observation using 5-MU. Although α_{1B}-AR expression could be represented as part of the low affinity binding population for both 5-MU and BMY 7378, previous reports have shown consistent 3-4 fold lower binding affinities of BMY 7378 for both recombinant and endogenously expressed α_{1A}-AR subtypes when compared to the α_{1B}-AR (Yoshio et al., 2001). The extremely low affinity population (K_{iL}) identified by BMY 7378 in our human macrophage system correlates well with the calculated BMY 7378 value for α_{1A}-AR subtypes in this previous report (Yoshio et al., 2001). At this time, an effective subtype-selective α_{1B}-AR antagonist is not available to validate (monocyte) or rule out (macrophage) α_{1B}-AR expression.

Parallel investigations characterized temporal increases in p38 MAPK activation from monocytes and macrophages concurrently treated with LPS and PE (fig 3). Significant increases over basal were shown for monocyte p38 MAPK activation starting at 15 min and peaking at 120 min. Significant phospho-p38 MAPK temporal increases were also observed using our macrophage cell model at 15 min followed by a shorter 30 min peak. Slower and persistent MAPK activation by $G\alpha_q$ coupled receptors have been shown to be β-arrestin dependent (Ahn et al., 2004). Moreover, direct interaction of the β-arrestin 1 isoform and MAPK kinase 3, which is specific for p38 MAPK activation has been previously described (McLaughlin et al., 2006). While there have been reports characterizing the importance of β-arrestin interactions for

JPET Fast Forward. Published on May 13, 2011 as DOI: 10.1124/jpet.110.178012
This article has not been copyedited and formatted. The final version may differ from this version.

internalization and recycling of α_{1A}-AR subtypes, β-arrestin dependent α_1-AR signaling pathways are not described in the literature (Pediani et al., 2005).

Our study goes further using pharmacological as well as molecular biological approaches to characterize the signal-transduction properties of this cooperative relationship between α_1-AR and TLR4 activation to generate a greater cytokine response. The synergistic IL-1β effect shown in our study is dependent upon α_1-AR stimulation as evidenced by a reversal of this response in the presence of a selective α_1-AR antagonist (fig 2). Moreover, inhibition of PKC using STS or Bis II blocked the synergistic increases in IL-1β production observed with PE plus LPS treatment to levels that were no different from cells treated with LPS alone (figs 2 and 5). Similarly, p38 MAPK inhibition decreased synergistic IL-1β production following PE plus LPS treatment to levels comparable with LPS only (fig 5). These results indicate that while PKC/p38 MAPK activation is not important for TLR4-initiated IL-1β generation the synergistic production of this pro-inflammatory cytokine with concurrent α_1-AR stimulation in monocytes and macrophages is PKC/p38 MAPK-dependent. These data are also the first to document functional α_1-AR expression on human monocytes and macrophages as well as linking their activation to an immunomodulatory increase in pro-inflammatory cytokine production. Interestingly, the homogeneous α_{1B}-AR subtype expression profile in monocytes changed to a heterogeneous population of α_{1A}- and α_{1D}-AR subtypes when differentiated into macrophages. Remarkably, the α_1-AR-mediated signaling pathway that regulates TLR4 cytokine production remained the same in both cell types. This observation points to the previously reported signaling redundancy as well as highly inducible nature of α_1-AR subtypes in immune cell populations (Rouppe van der Voort et al., 1999; Rouppe van der Voort et al., 2000; Heijnen et al., 2002).

TLR4 mediated increases in IL-1β from human lymphocytes has been documented to occur through both pre- and post-transcriptional mechanisms (Netea et al., 2009). In cardiac myocytes, α_1-AR activation promotes the generation of IL-6 through a combination of transcription factor activation and increased mRNA stability (Perez et al., 2009). Similar mechanisms are likely occurring in our studies since quantities of both pro- and bioactive IL-1β are increased with concurrent α_1-AR and TLR4 activation, indicating the generation of new protein. TLR4 effector pathways are typically linked to the myeloid differentiation primary-response protein 88 (MyD88) signaling complex, which activates the nuclear factor kappa-light-chain-enhancer of activated B cells (NF-κB) to regulate IL-1β transcription (Akira and Takeda, 2004). While it is possible that positive α_1-AR regulation of TLR4 signaling occurs upstream of PKC and p38 MAPK, the majority of literature points to alterations in the NF-κB or MAPK signaling pathways. However, increased Ca^{2+} concentrations in macrophages has been shown to initiate MyD88 signaling through direct interaction and phosphorylation of transforming growth factor β-activated kinase (TAK)1, an important activator of both NF-κB and p38 MAPK pathways (Liu et al., 2008b). As a result, $G\alpha_q$-mediated enhanced Ca^{2+} levels initiated by α_1-AR stimulation could activate p38 MAPK, which was shown to be necessary for the potentiated IL-1β response in our systems. Conversely, TLR4 inflammatory signaling can also occur independent of NF-κB through p38 MAPK-dependent mobilization of activator protein-1 (AP-1) or ETS domain-containing protein Elk-1 (ELK-1) transcription factors (Hodgkinson et al., 2008; Smolinska et al., 2008). Activated p38 MAPK shown in our results may be positively regulating TLR4-initiated IL-1β production through these surrogate transcription factors. Alternatively, α_1-AR-mediated phospho-p38 MAPK characterized in our studies could have direct positive effects on

NF-κB activity by enhancing inhibitor of κB (IκB) degradation or by mediating acetylation of the RelA transcription factor subunit (Liu et al., 2008a; Pan et al., 2010).

Increased IL-1β from innate immunocompetent cells have been implied in the pathogenesis of rheumatoid arthritis, type 1 diabetes, multiple sclerosis and Alzheimer's disease (Licastro et al., 2000; Audoy-Remus et al., 2008; Capellino and Straub, 2008; Bradshaw et al., 2009). Therefore, α_1-AR modulation of TLR4 signaling characterized in our investigations may prove to be a useful therapeutic strategy for the management of human diseases with known chronic inflammatory etiologies.

Acknowledgments:

The authors would like to thank Brett McGregor for his technical support as well as Julie Horn and Deb Kroese for their administrative assistance.

Authorship Contributions:

Participated in research design: Grisanti, Combs, Porter

Conducted experiments: Grisanti, Woster, Dahlman

Contributed new reagents or analytic tools: Dahlman, Sauter, Combs

Performed data analysis: Grisanti, Woster, Combs, Porter

Wrote or contributed to the writing of the manuscript: Grisanti, Sauter, Combs, Porter

References:

Ahn S, Shenoy SK, Wei H, and Lefkowitz RJ (2004) Differential kinetic and spatial patterns of β-arrestin and G protein-mediated ERK activation by the angiotensin II receptor. *J Biol Chem* **279**:35518-35525.

Akira S and Takeda K (2004) Toll-like receptor signalling. *Nat Rev Immunol* **4**:499-511.

Audoy-Remus J, Richard J-F, Soulet D, Zhou H, Kubes P, and Vallieres L (2008) Rod-shaped monocytes patrol the brain vasculature and give rise to perivascular macrophages under the influence of proinflammatory cytokines and angiopoietin-2. *J Neurosci* **28**:10187-10199.

Bradshaw EM, Raddassi K, Elyaman W, Orban T, Gottlieb PA, Kent SC, and Hafler DA (2009) Monocytes from patients with type 1 diabetes spontaneously secrete proinflammatory cytokines inducing Th17 cells. *J Immunol* **183**:4432-4439.

Brosnan CF, Goldmuntz EA, Cammer W, Factor SM, Bloom BR, and Norton WT (1985) Prazosin, an α_1-adrenergic receptor antagonist, suppresses experimental autoimmune encephalomyelitis in the Lewis rat. *Proc Natl Acad Sci U S A* **82**:5915-5919.

Calcagni E and Elenkov I (2006) Stress system activity, innate and T helper cytokines, and susceptibility to immune-related diseases. *Ann N Y Acad Sci* **1069**:62-76.

Capellino S and Straub R (2008) Neuroendocrine immune pathways in chronic arthritis. *Best Pract Res Clin Rheumatol* **22**:285-297.

Casale TB and Kaliner M (1984) Demonstration that circulating human blood cells have no detectable α_1-adrenergic receptors by radioligand binding analysis. *J Allergy Clin Immunol* **74**:812-818.

Elenkov IJ, Kvetnansky R, Hashiramoto A, Bakalov VK, Link AA, Zachman K, Crane M, Jezova D, Rovensky J, Dimitrov MA, Gold PW, Bonini S, Fleisher T, Chrousos GP, and Wilder RL (2008) Low- versus high-baseline epinephrine output shapes opposite innate cytokine profiles: Presence of Lewis- and Fischer-like neurohormonal immune phenotypes in humans? *J Immunol* **181**:1737-1745.

Farmer P and Pugin J (2000) β-Adrenergic agonists exert their "anti-inflammatory" effects in monocytic cells through the IκB/NF-κB pathway. *Am J Physiol Lung Cell Mol Physiol* **279**:L675-L682.

Felsner P, Hofer D, Rinner I, Porta S, Korsatko W, and Schauenstein K (1995) Adrenergic suppression of peripheral blood T cell reactivity in the rat is due to activation of peripheral α_2-receptors. *J Neuroimmunol* **57**:27-34.

Flierl MA, Rittirsch D, Nadeau BA, Chen AJ, Sarma JV, Zetoune FS, McGuire SR, List RP, Day DE, Hoesel LM, Gao H, Van RN, Huber-Lang MS, Neubig RR, and Ward PA (2007) Phagocyte-derived catecholamines enhance acute inflammatory injury. *Nature* **449**:721-725.

Goetz AS, Kng HK, Ward SDC, True TA, Rimele TJ, and Saussy DL, Jr. (1995) BMY 7378 is a selective antagonist of the D subtype of α_1-adrenoceptors. *Eur J Pharmacol* **272**:R5-R6.

Grisanti LA, Evanson J, Marchus E, Jorissen H, Woster AP, DeKrey W, Sauter ER, Combs CK, and Porter JE (2010) Pro-inflammatory responses in human monocytes are β_1-adrenergic receptor subtype dependent. *Mol Immunol* **47**:1244-1254.

Grisanti LA, Perez DM, and Porter JE (in press) Modulation of immune cell function by α_1-adrenergic receptor activation, in *Advances in adrenergic receptor biology* (Wang Q ed), Elsevier Publishing, United Kingdom.

Gross G, Hanft G, and Rugevics C (1988) 5-Methyl-urapidil discriminates between subtypes of the α_1-adrenoceptor. *Eur J Pharmacol* **151**:333-335.

Guimarães S and Moura D (2001) Vascular adrenoceptors: An update. *Pharmacol Rev* **53**:319-356.

Hasko G, Elenkov IJ, Kvetan V, and Vizi ES (1995) Differential effect of selective block of α_2-adrenoreceptors on plasma levels of tumour necrosis factor-α, interleukin-6 and corticosterone induced by bacterial lipopolysaccharide in mice. *J Endocrinol* **144**:457-462.

Heijnen CJ, Rouppe van der Voort C, van de Pol M, and Kavelaars A (2002) Cytokines regulate α_1-adrenergic receptor mRNA expression in human monocytic cells and endothelial cells. *J Neuroimmunol* **125**:66-72.

Heijnen CJ, Rouppe van der Voort C, Wulffraat N, van der Net J, Kuis W, and Kavelaars A (1996) Functional α_1-adrenergic receptors on leukocytes of patients with polyarticular juvenile rheumatoid arthritis. *J Neuroimmunol* **71**:223-226.

Hodgkinson CP, Patel K, and Ye S (2008) Functional Toll-like receptor 4 mutations modulate the response to fibrinogen. *Thromb Haemost* **100**:301-307.

Jensen BC, Swigart PM, and Simpson PC (2009) Ten commercial antibodies for alpha-1-adrenergic receptor subtypes are nonspecific. *Naunyn Schmiedebergs Arch Pharmacol* **379**:409-412.

Johnson JD, Campisi J, Sharkey CM, Kennedy SL, Nickerson M, Greenwood BN, and Fleshner M (2005) Catecholamines mediate stress-induced increases in peripheral and central inflammatory cytokines. *Neuroscience* **135**:1295-1307.

Licastro F, Pedrini S, Caputo L, Annoni G, Davis LJ, Ferri C, Casadei V, and Grimaldi LM (2000) Increased plasma levels of interleukin-1, interleukin-6 and α-1-antichymotrypsin in patients with Alzheimer's disease: Peripheral inflammation or signals from the brain? *J Neuroimmunol* **103**:97-102.

Liu S, Feng G, Wang GL, and Liu GJ (2008a) p38MAPK inhibition attenuates LPS-induced acute lung injury involvement of NF-κB pathway. *Eur J Pharmacol* **584**:159-165.

Liu X, Yao M, Li N, Wang C, Zheng Y, and Cao X (2008b) CaMKII promotes TLR-triggered proinflammatory cytokine and type I interferon production by directly binding and activating TAK1 and IRF3 in macrophages. *Blood* **112**:4961-4970.

Maestroni GJ (2000) Dendritic cell migration controlled by α_{1b}-adrenergic receptors. *J Immunol* **165**:6743-6747.

McLaughlin NJD, Banerjee A, Kelher MR, Gamboni-Robertson F, Hamiel C, Sheppard FR, Moore EE, and Silliman CC (2006) Platelet-activating factor-induced clathrin-mediated endocytosis requires β-arrestin-1 recruitment and activation of the p38 MAPK signalosome at the plasma membrane for actin bundle formation. *J Immunol* **176**:7039-7050.

Netea MG, Nold-Petry CA, Nold MF, Joosten LA, Opitz B, van der Meer JH, van de Veerdonk FL, Ferwerda G, Heinhuis B, Devesa I, Funk CJ, Mason RJ, Kullberg BJ, Rubartelli A, van der Meer JW, and Dinarello CA (2009) Differential requirement for the activation of the inflammasome for processing and release of IL-1β in monocytes and macrophages. *Blood* **113**:2324-2335.

Pan WW, Li JD, Huang S, Papadimos TJ, Pan ZK, and Chen LY (2010) Synergistic activation of NF-κB by bacterial chemoattractant and TNFα is mediated by p38 MAPK-dependent RelA acetylation. *J Biol Chem* **285**:34348-34354.

Pediani JD, Colston JF, Caldwell D, Milligan G, Daly CJ, and McGrath JC (2005) β-arrestin-dependent spontaneous α_{1a}-adrenoceptor endocytosis causes intracellular transportation of α-blockers via recycling compartments. *Mol Pharmacol* **67**:992-1004.

Perez DM, Papay RS, and Shi T (2009) α_1-Adrenergic receptor stimulates interleukin-6 expression and secretion through both mRNA stability and transcriptional regulation: Involvement of p38 mitogen-activated protein kinase and nuclear factor-κB. *Mol Pharmacol* **76**:144-152.

Romero-Sandoval EA, McCall C, and Eisenach JC (2005) α2-Adrenoceptor stimulation transforms immune responses in neuritis and blocks neuritis-induced pain. *J Neurosci* **25**:8988-8994.

Rouppe van der Voort C, Kavelaars A, van de Pol M, and Heijnen CJ (1999) Neuroendocrine mediators up-regulate α_{1b}- and α_{1d}-adrenergic receptor subtypes in human monocytes. *J Neuroimmunol* **95**:165-173.

Rouppe van der Voort C, Kavelaars A, van de Pol M, and Heijnen CJ (2000) Noradrenaline induces phosphorylation of ERK-2 in human peripheral blood mononuclear cells after induction of α_1-adrenergic receptors. *J Neuroimmunol* **108**:82-91.

Smolinska MJ, Horwood NJ, Page TH, Smallie T, and Foxwell BMJ (2008) Chemical inhibition of Src family kinases affects major LPS-activated pathways in primary human macrophages. *Mol Immunol* **45**:990-1000.

Spengler R, Allen R, Remick D, Strieter R, and Kunkel S (1990) Stimulation of α-adrenergic receptor augments the production of macrophage-derived tumor necrosis factor. *J Immunol* **145**:1430-1434.

Tsuchiya S, Kobayashi H, Goto Y, Okumura H, Nakae S, Konno T, and Tada K (1982) Induction of maturation in cultured human monocytic leukemia cells by a phorbol diester. *Cancer Res* **42**:1530-1536.

Whitmarsh A, Shore P, Sharrocks A, and Davis R (1995) Integration of MAP kinase signal transduction pathways at the serum response element. *Science* **269**:403-407.

Yoshio R, Taniguchi T, Itoh H, and Muramatsu I (2001) Affinity of serotonin receptor antagonists and agonists to recombinant and native α_1-adrenoceptor subtypes. *Jpn J Pharmacol* **86**:189-195.

Footnotes:

a) Financial Support:

This study was supported by the National Science Foundation [Grant 0235146]; the National Institutes of Health [Grants GM066726, DK62865]; the National Institutes of Health Centers of Biomedical Research Excellence (COBRE) program [Grant RR016471]; and the North Dakota Experimental Program to Stimulate Competitive Research (EPSCoR) program through the National Science Foundation [Grant EPS-0447679] (to J.E.P).

b) Unnumbered Footnote:

A preliminary report of these findings were presented at the *Annual Meeting of the American Society for Pharmacology and Experimental Therapeutics*; April 18-22, 2009, New Orleans, LA. American Society for Pharmacology and Experimental Therapeutics, Bethesda, MD.

c) Reprint Requests:

James E. Porter

Department of Pharmacology, Physiology and Therapeutics

University of North Dakota School of Medicine and Health Sciences

501 North Columbia Road

Room 3700, Stop 9037

Grand Forks, ND 58202-9037

e-mail: james.porter@med.und.edu

d) Numbered Footnotes:

[1]The Integrative and Organ Systems Pharmacology internship of L.A.G. at the University of Nebraska Medical Center was support by the National Institutes of Health [Grant R25GM074089]

[2]A.P.W. current address is: South Dakota State University, Psychology Department, Box 504, Brookings, SD 57007.

JPET Fast Forward. Published on May 13, 2011 as DOI: 10.1124/jpet.110.178012
This article has not been copyedited and formatted. The final version may differ from this version.

Legends for Figures:

Figure 1: *α_1-AR modulation of IL-1β production from LPS challenged primary human monocytes.* **Panel A**, Representative immunoblot of resolved total cell lysates from isolated primary human monocytes. The 42 kDa actin band is shown as a loading control. **Panel B**, Quantitative analysis of all immunoblots (n=7) showed increased expression of IL-1β from cells treated with LPS only (8.9±3.1 fold). Additionally, there was a synergistic increase in IL-1β generation from cells treated with PE plus LPS (31.0±5.8 fold). There were no differences in IL-1β production from cells treated with PE (1.0±0.6 fold) alone. (★, $p < 0.05$ vs. control; #, $p < 0.05$ vs. LPS)

Figure 2: *α_1-AR mediated synergistic IL-1β production from a human monocyte cell line*. **Panel A**, Representative immunoblot of resolved THP-1 total cell lysates. The 42 kDa actin band is shown as a loading control. **Panel B**, Quantitative analysis of all immunoblots (n=5) showed increased IL-1β expression from monocytes treated with LPS alone (3.3±0.8 fold). There was a synergistic increase in IL-1β generated from cells treated with PE plus LPS (8.7±3.0 fold). There were decreased IL-1β levels from monocytes pretreated with BE 2254 (3.4±1.0 fold) or STS (2.8±0.4 fold). There were no IL-1β differences from cells treated with PE (1.0±0.6 fold), BE 2254 (0.9±0.3 fold) or STS (0.9±0.2 fold) alone. **Panel C**, Quantitative ELISA analysis for secreted amounts of IL-1β from THP-1 cells (n=5). There was increased IL-1β secretion from monocytes treated with LPS only (23.6±4.2 pg/mL). There were also synergistic IL-1β increases from monocytes treated with PE plus LPS (59.5±11.1 pg/mL). There were no differences in IL-1β secreted from cells treated with PE alone (8.2±0.9 pg/mL) compared to basal (2.3±0.2 pg/mL). (★, $p < 0.05$ vs. control; #, $p < 0.05$ vs. LPS; °, $p < 0.05$ vs. PE+LPS)

Figure 3: *Temporal p38 MAPK responses in monocytes/macrophages initiated by concurrent α_1-AR and TLR4 stimulation.* **Panel A**, Representative immunoblot of resolved THP-1 total cell lysates incubated concurrently with PE and LPS. **Panel B**, Quantitative analysis of all immunoblots (n=3) showed increased phosphorylated p38 MAPK from monocytes treated for 30 (4.2±0.6 fold), 60 (4.6±1.3 fold) and 120 min (8.2±0.6 fold). There were no differences in activated p38 MAPK generated from monocytes treated for 15 (2.4±0.3 fold) and 180 min (2.1±0.4 fold). **Panel C**, Representative immunoblot (n=3) of resolved THP-1 total cell lysates incubated with LPS alone. **Panel D**, Representative immunoblot of resolved PMA differentiated THP-1 total cell lysates incubated concurrently with PE and LPS. **Panel E**, Quantitative analysis of all immunoblots (n=3) showed increased phosphorylated p38 MAPK from macrophages treated for 15 (7.7±1.2 fold) and 30 min (10.7±1.6 fold). There were no differences in activated p38 MAPK generated from macrophage cells treated for 5 (1.5±0.6 fold), 60 (3.4±1.0 fold) and 120 min (3.2±0.2 fold). **Panel F**, Representative immunoblot (n=3) of resolved PMA differentiated THP-1 total cell lysates incubated with LPS alone. In all immunoblots, the 43 kDa non-phosphorylated p38 MAPK band is shown as a loading control. (★, $p < 0.05$ vs. control)

Figure 4: *Selective inhibition of α_1-AR mediated PKC/p38 MAPK activation in LPS challenged monocytes/macrophages.* **Panel A**, Representative immunoblot of resolved THP-1 total cell lysates. **Panel B**, Quantitative analysis of all immunoblots (n=3) showed phosphorylated p38 MAPK increases from monocytes treated with PE plus LPS (7.2±1.1 fold). There were no differences from control for any other treatments. **Panel C**, Representative immunoblot of resolved PMA differentiated THP-1 total cell lysates. **Panel D**, Quantitative analysis of all

immunoblots (*n*=3) showed increases in phosphorylated p38 MAPK from macrophages treated with PE plus LPS (3.1±0.6 fold). There were no changes from control for any other treatments. The 43 kDa non-phosphorylated p38 MAPK band is shown as a loading control for all immunoblots. (★, $p < 0.05$ vs. control)

Figure 5: *PKC/p38 MAPK activation is associated with α_1-AR mediated synergistic IL-1β production from LPS challenged monocytes/macrophages.* **Panel A**, Representative immunoblot of resolved THP-1 total cell lysates. **Panel B**, Quantitative analysis of all immunoblots (*n*=3) showed increases in generated IL-1β from monocytes treated with LPS alone (3.8±0.9 fold). There was synergistic IL-1β production from monocytes treated with PE plus LPS (8.7±3.0 fold). Monocytes pretreated with SB 203580 or Bis II showed differences in generated IL-1β (3.9±1.0 and 3.1±1.2 fold, respectively). There were no IL-1β changes after treatment with PE (1.3±0.2 fold), SB 203580 (0.7±0.3 fold) or Bis II (1.0±0.1 fold) only. **Panel C**, Representative immunoblot of resolved PMA differentiated THP-1 total cell lysates. **Panel D**, Quantitative analysis of all immunoblots (*n*=3) showed increases in IL-1β generated from macrophages treated with LPS alone (1.8±0.4 fold). There was synergistic IL-1β production from macrophages treated with PE plus LPS (3.3±0.5 fold). Macrophages pretreated with SB 203580 or Bis II showed changes in IL-1β levels (1.5±0.1 and 1.2±0.3 fold, respectively). There were no IL-1β differences produced from macrophages treated with PE (1.3±0.1 fold), SB 203580 (0.7±0.1) or Bis II (0.4±0.1 fold) only. The 42 kDa actin band is shown as a loading control in all immunoblots. (★, $p < 0.05$ vs. control; #, $p < 0.05$ vs. LPS; °, $p < 0.05$ vs. PE+LPS)

Figure 6: *p38 MAPK activation is necessary for the α_1-AR synergistic modulation of IL-1β production.* **Panel A**, Representative immunoblot of resolved THP-1 total cell lysates over expressing the empty vector or DN p38 MAPK plasmid constructs. The 42 kDa actin band is shown as a loading control. **Panel B**, Quantitative analysis of all immunoblots (n=3), normalized to basal levels of cells transfected with empty vector showed increases in IL-1β generated from similarly transfected cells treated with PE plus LPS (7.2±2.5 fold). There were no IL-1β differences in DN p38 MAPK transfected cells observed from control (0.8±0.4 fold) or PE plus LPS treatments (1.1±0.2 fold). (★, $p < 0.05$ vs. empty vector control)

Figure 7: *Immunoblot analysis of α_1-AR protein expression from THP-1 cell lysates.* Independent, untreated THP-1 cell lysate preparations (n=3) were resolved and probed with antibodies that recognize the α_{1A}- or α_{1B}-AR subtypes. In all preparations the putative specific band for the α_{1B}-AR was observed around the predicted ≈ 88 kDa size. No specific α_{1A}-AR protein band was detected in any independent monocyte preparation.

JPET Fast Forward. Published on May 13, 2011 as DOI: 10.1124/jpet.110.178012
This article has not been copyedited and formatted. The final version may differ from this version.

Table 1:

Equilibrium dissociation constants (K_i) of α_1-AR antagonists for ^{125}I-HEAT specific binding sites on human monocytes and macrophages.

Monocyte (THP-1)				
nM (*n*)	BE 2254 (3)	5-MU (4)	WB-4101 (4)	BMY 7378 (4)
K_i	5.3±1.0	10864±1920	435±85	1079±212
Macrophage (PMA Differentiated THP-1)				
K_i	*11.0±0.0			
K_{iH}		1.3±4.6		1.0±0.9
K_{iL}		85507±4332		1371±605

Mean values ± S.E.M. (in nM) calculated from individually generated inhibition curves of *n* competitive binding assays. For each individual experiment, the fitted iterative non-linear regression curve that best represented the data (*i.e.*, one vs. two-site fit) was determined using a partial *f* test ($p < 0.05$). *n=1.

Figure 1

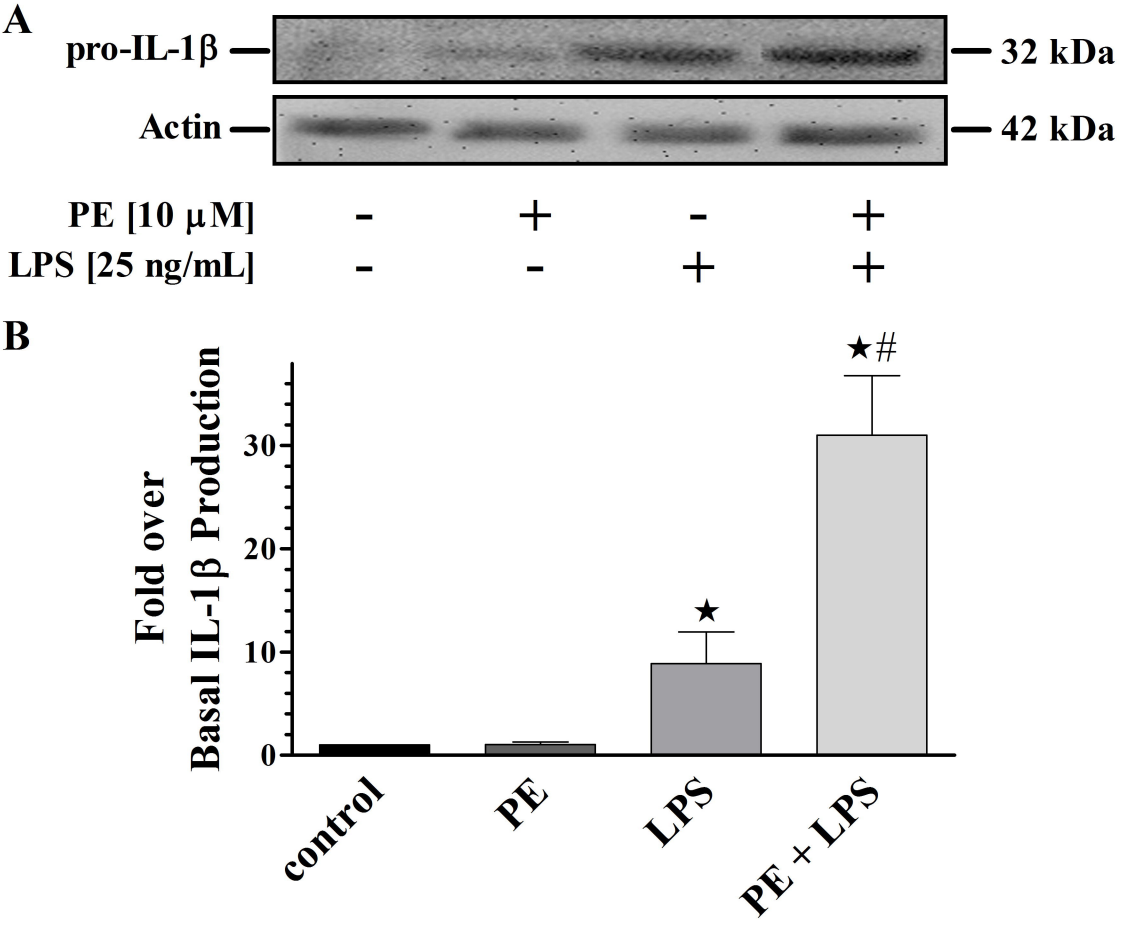
A
pro-IL-1β
32 kDa
Actin
42 kDa
PE [10 μM]
LPS [25 ng/mL]
B
Fold over Basal IL-1β Production
0
10
20
30
★
★#
control
PE
LPS
PE + LPS

Figure 2

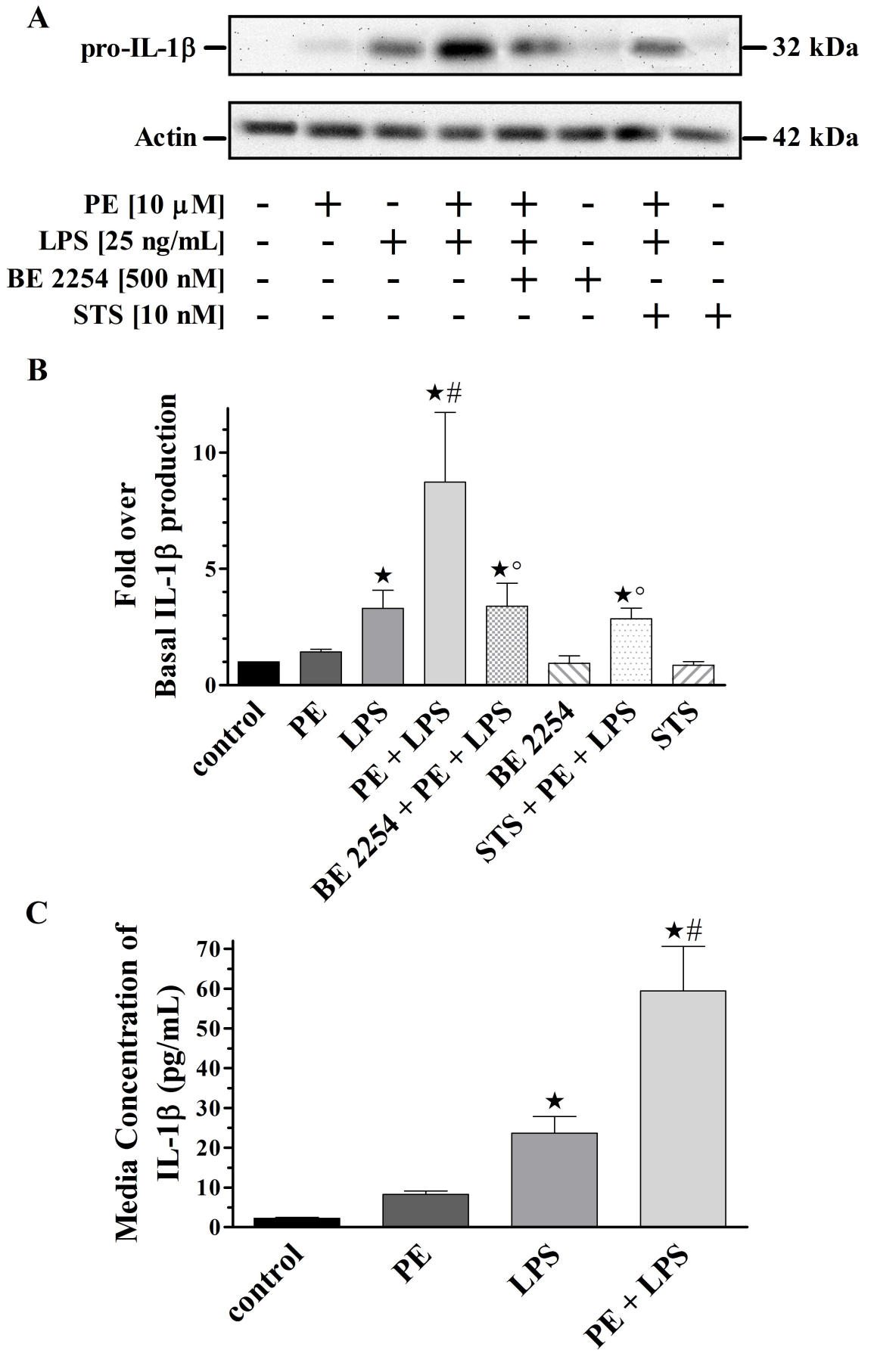
A
pro-IL-1β
32 kDa
Actin
42 kDa
PE [10 μM] - + - + + - + -
LPS [25 ng/mL] - - + + + - + -
BE 2254 [500 nM] - - - - + + - -
STS [10 nM] - - - - - - + +
B
Fold over Basal IL-1β production
0
5
10
★
★°
★°
★#
control
PE
LPS
PE + LPS
BE 2254 + PE + LPS
BE 2254
STS + PE + LPS
STS
C
Media Concentration of IL-1β (pg/mL)
0
10
20
30
40
50
60
70
★
★#
control
PE
LPS
PE + LPS

Figure 3

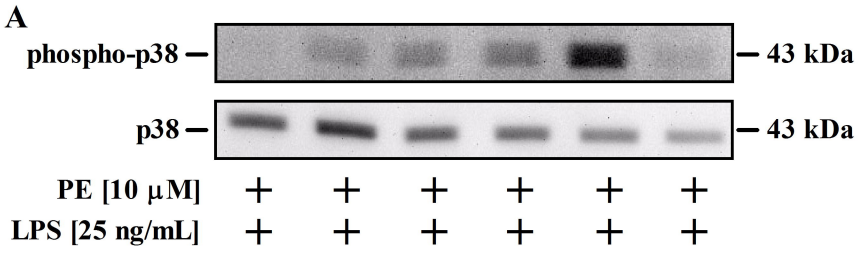

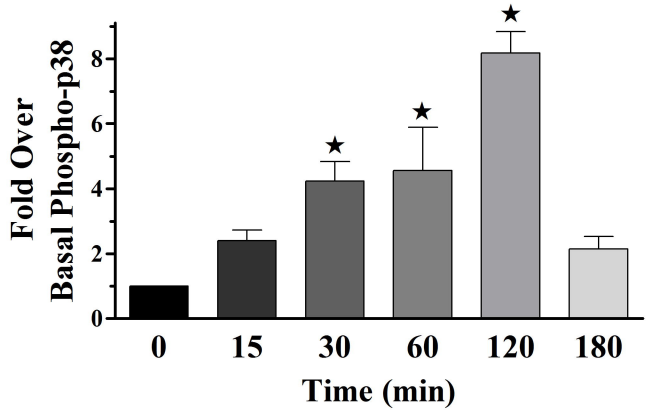

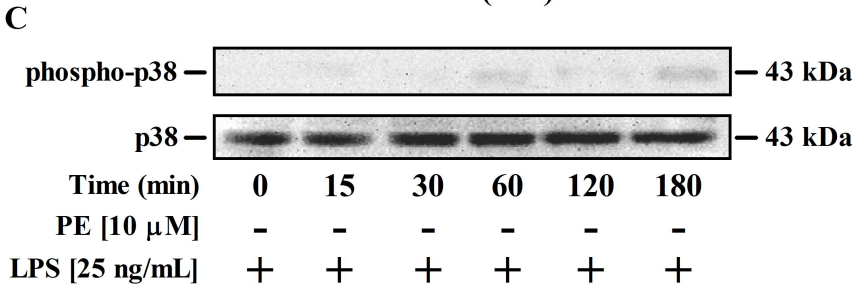

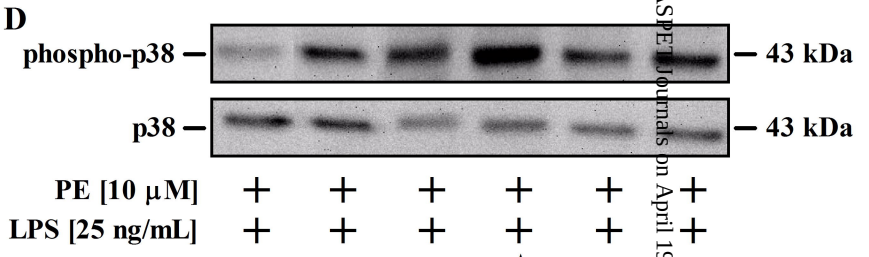

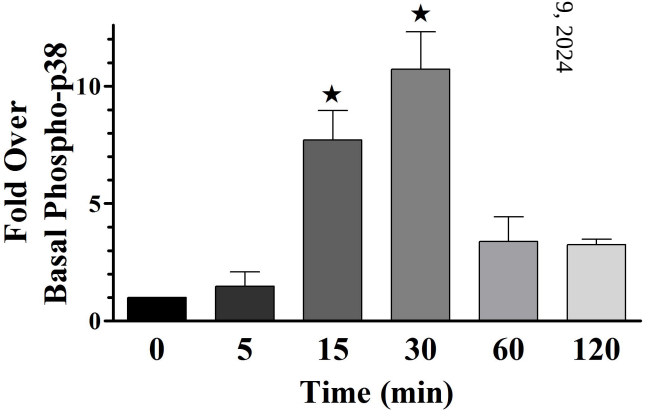

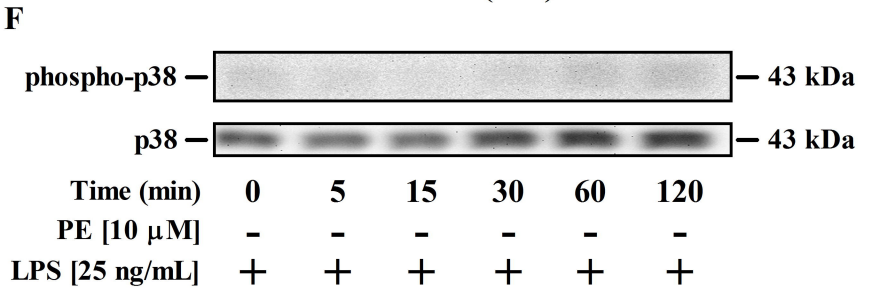

Figure 4

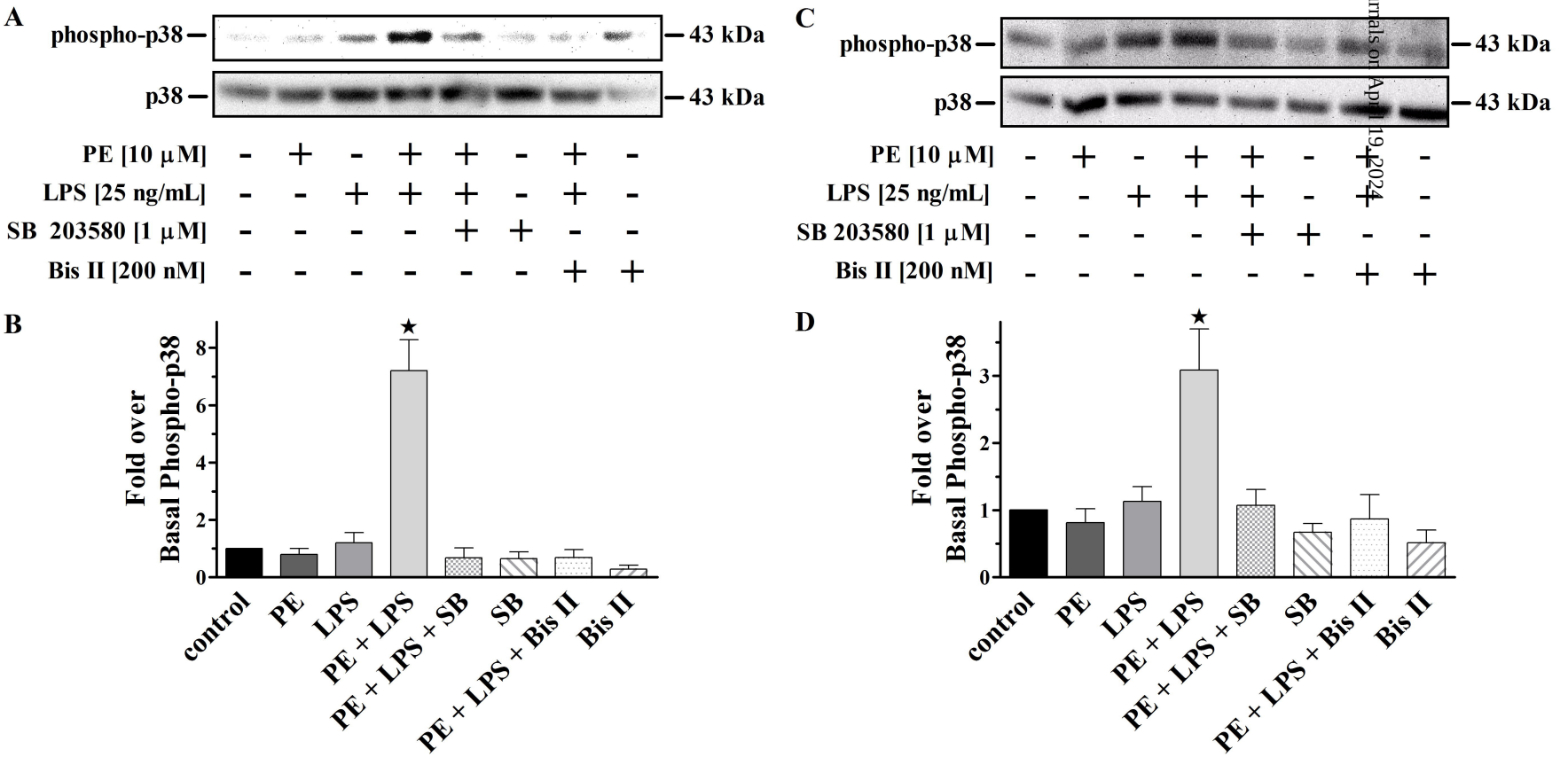

Figure 5

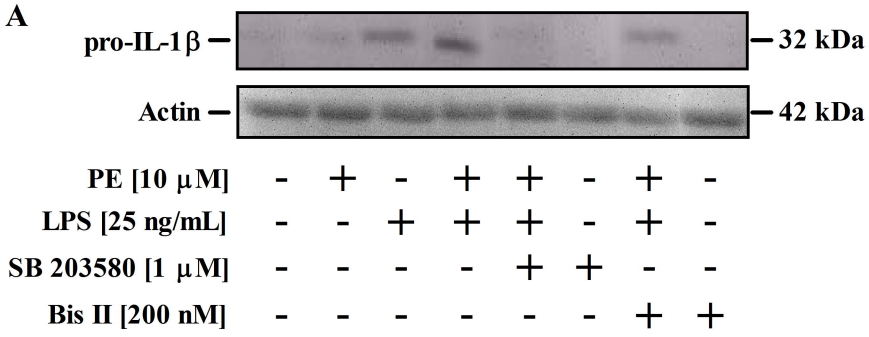

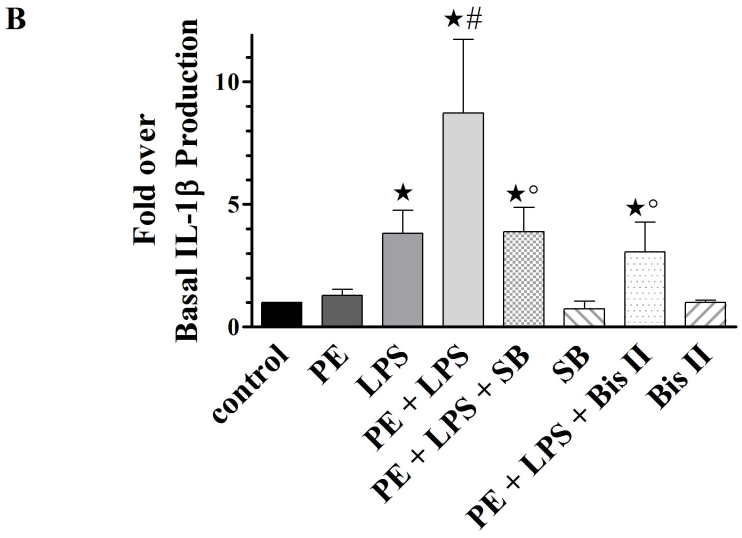

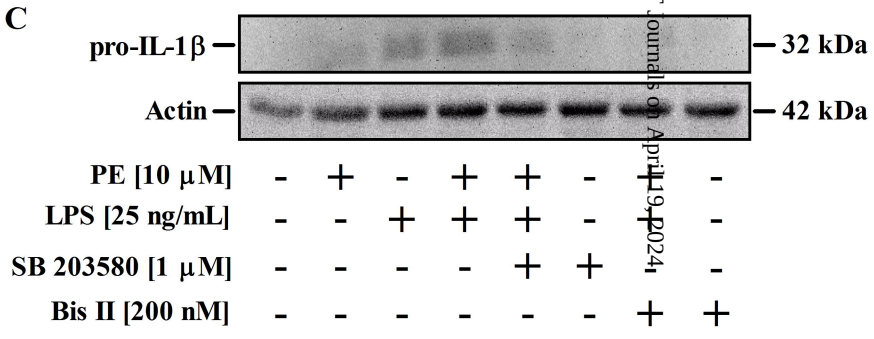

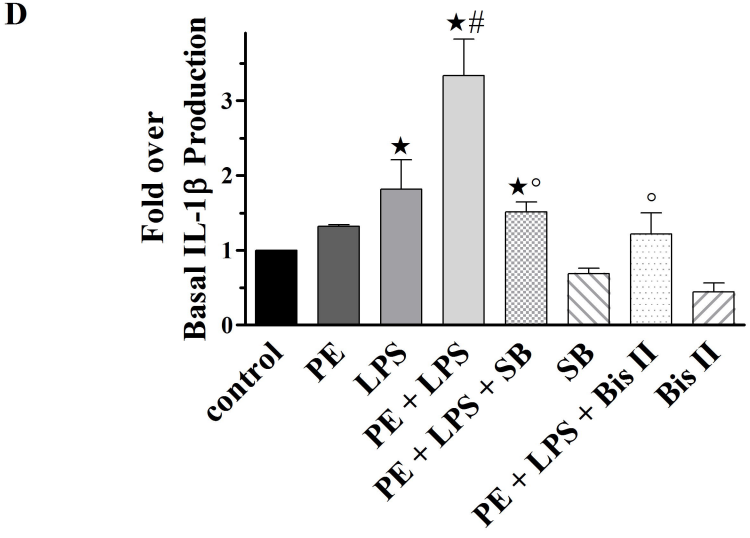

Figure 6

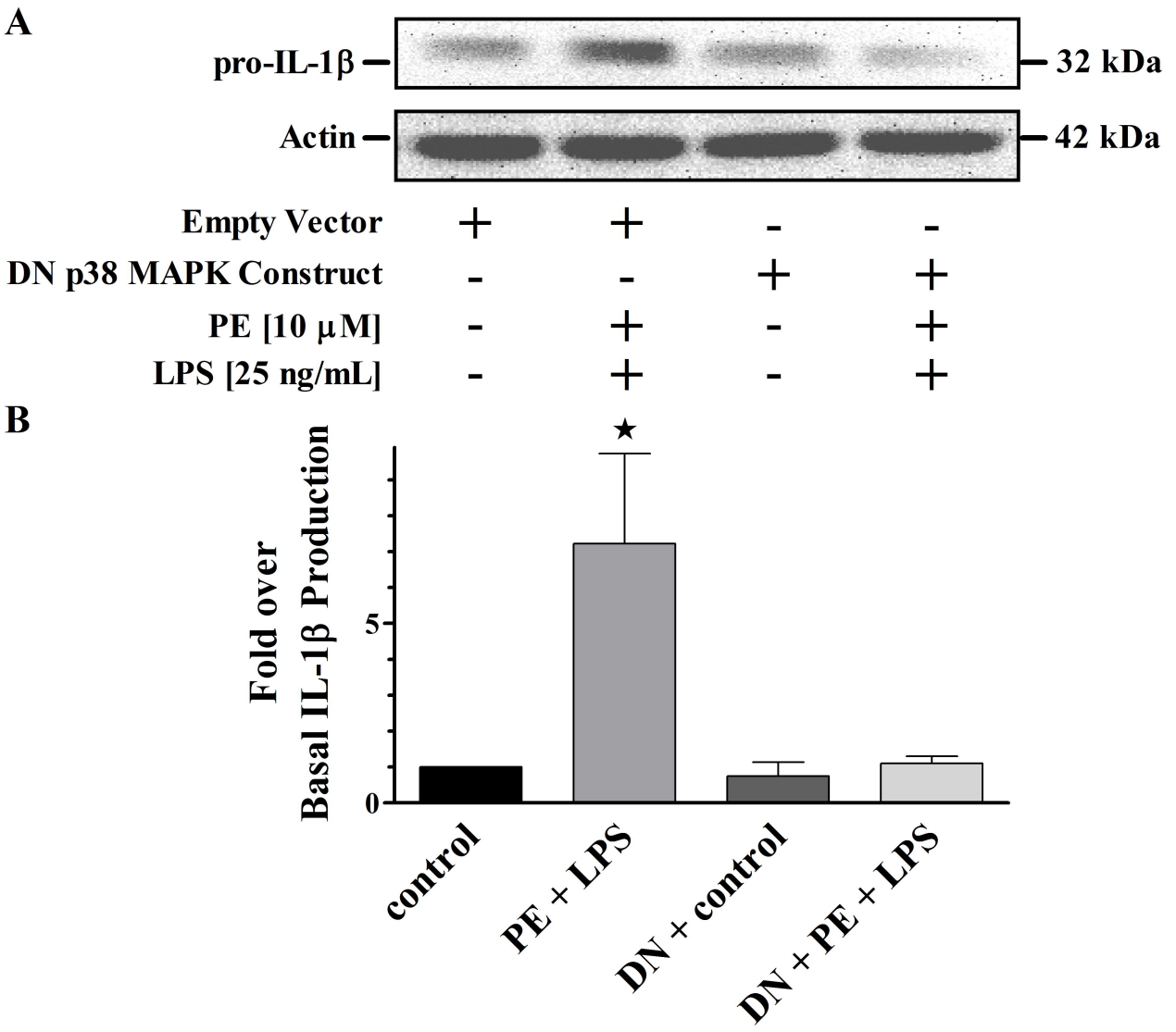
A
pro-IL-1β
32 kDa
Actin
42 kDa
Empty Vector + + - -
DN p38 MAPK Construct - - + +
PE [10 μM] - + - +
LPS [25 ng/mL] - + - +
B
Fold over Basal IL-1β Production
★
5
0
control
PE + LPS
DN + control
DN + PE + LPS

Figure 7